X-rays and Regions of Star Formation: a Combined ROSAT/ISO Study of The ρ Ophiuchi Cloud

Nicolas Grosso and Thierry Montmerle
Service d'Astrophysique, Centre d'Études de Saclay, 91191 Gif-sur-Yvette Cedex, France

Sylvain Bontemps
Observatoire de Bordeaux, BP 89, 33270 Floirac, France

Philippe André
Service d'Astrophysique, Centre d'Études de Saclay, 91191 Gif-sur-Yvette Cedex, France

Eric D. Feigelson
Departement of Astronomy and Astrophysics, Pennsylvania State University, University Park, PA 1680, USA

ABSTRACT

We have obtained two deep exposures of the ρ Oph cloud core region (d$\sim$160pc) with the *ROSAT High Resolution Imager* (core A: 51 ksec, core F: 77 ksec). The improved angular accuracy (1″–6″) with respect to previous recent observations (*ROSAT PSPC*, Casanova *et al.* 1995; and *ASCA*, Kamata *et al.* 1997) allows the removal of positional ambiguities for the detected sources. We also cross-correlate the X-ray positions with IR sources found in the *ISO/ISOCAM* survey of the same region at 6.7 and 15 μm, in addition to sources (optical and IR) known from ground-based observations, which are young stars (T Tauri Stars, with and without IR excess/circumstellar disks, and protostars). We thus obtain the best-studied sample of X-ray emitting stars in a star-forming region, which confirms and significantly improves the results obtained previously.

We confirm that essentially all young stars are X-ray emitters, with a large majority of TTSs, and that a strong correlation exists between their stellar luminosities and their X-ray luminosities. Most of the new TTSs with IR excess discovered by *ISOCAM* are not detected, however, which is explained by the fact that their X-ray luminosities "predicted" on the basis of this correlation are too faint to be detected by the *HRI*. Protostars are not detected with the *HRI*, with the exception of the protostar YLW15, which was detected in the course of an extraordinarily powerful flare.

We will discuss the susbtantial improvements that *XMM* will bring to the field:
• greater capability to overcome high extinctions, thanks to the increase in sensitivity and the access to the 5-10 keV energy range, hence the possibility to detect more faint *ISOCAM* sources, protostars, and perhaps brown dwarfs;
• capability to do spectral studies at high resolution, allowing detailed studies of the plasma composition and temperature(s), and of the extinction along the line-of-sight.

1. Introduction

Since the early 1980's with the *Einstein* satellite observations, regions of star formation are known to be X-ray emitters. X-ray are emitted by T Tauri Stars (hereafter TTSs), and also by Protostars as recently discovered both by *ROSAT* and *ASCA* (Casanova *et al.* 1995; Koyama *et al.* 1996; Grosso *et al.* 1997; Kamata *et al.* 1997). TTSs and protostars are low mass Young Stellar Objects (hereafter YSOs): 10^4–10^5 years old for protostars, and 1–10 Million years old for TTSs (André & Montmerle 1994). Motivations for a combined X-ray and Infra-Red (hereafter IR) study are twofold. First, YSOs are embedded in their parent cloud, with a high visual extinction, and both IR and X-ray observations can see through the dust. Second, IR observations detect protostars and TTSs with IR excess, but can not distinguish between field stars and TTSs without IR excess (i.e. TTSs without a thick circumstellar disk). This distinction can be done using X-rays because for a given bolometric luminosity TTSs are more X-ray luminous than Main-Sequence Stars. Here, we will take as an illustration the nearby ρ Ophiuchi star-forming region, located $\sim$ 160 pc from the Sun (Fig. 1-*left*). In this study the mid-IR data come from Bontemps *et al.* (1998), who have studied the stellar content of the *ISOCAM* survey of the ρ Ophiuchi cloud.

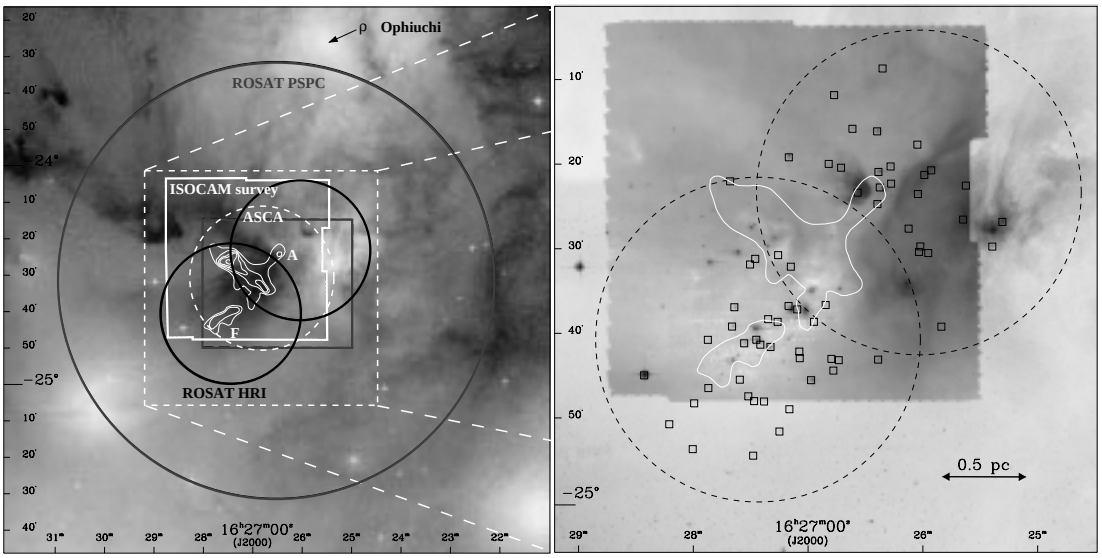

Fig. 1.— *(left)* ρ Ophiuchi dark cloud X-ray fields. Two degree diameter *ROSAT PSPC* field of view, and $35' \times 35'$ field studied by Casanova *et al.* (1995); $40'$ diameter *ROSAT HRI* fields of view; *ASCA* field of view from Kamata *et al.* (1997); *ISOCAM* survey field (Nordh, Olofsson *et al.*). The background image of the ρ Ophiuchi star-forming region is taken from the Digitized Sky Survey; the contrast was enhanced with gaussian histogram specification (Canzian 1997). Regions of high visual extinction are clearly visible. DCO^+(J=2-1) contour map of Loren *et al.* (1990) shows the position of dense molecular cores A and F. *(right)* X-ray sources in the *ROSAT HRI* fields. The *ISOCAM* map (LW2 filter image [5–8.5 μm], plus LW3 filter image [12–18 μm]; Abergel *et al.* 1996) is merged with the background optical image taken from the Digitized Sky Survey. First level of DCO^+(J=2-1) contour map of Loren *et al.* (1990) are shown ($T_A^\star$ = 0.4K). One *ISOCAM* map pixel is $6''$. The positions of the *HRI* X-ray sources are marked by squares. Typical X-ray error positions range between $1''$–$6''$, which allows us to find counterparts without ambiguity.

2. ROSAT X-ray and ISOCAM IR sources in the ρ Ophiuchi cloud

Casanova *et al.* (1995) observed this star-forming region with the *ROSAT Position Sensitive Proportional Counter* (*PSPC*). We have done a follow up of this observation with the *ROSAT High Resolution Imager* (*HRI*). We have two observation fields centered on DCO^+ dense cores A and F (Loren 1990, see Fig. 1). Core A field was observed between 1995 August 29 and 1995 September 12 with a total exposure of 51,259 sec. Core F field was observed three times : 1995 March 9–14 (12,473 sec), 1995 August 18–20 (27,540 sec), and 1996 September 7–11 (37,169 sec); these three partial exposures total 77,182 sec.
We found 63 X-ray sources ($> 3.25\sigma$), of which 55 are identified with IR or optical stars. Our X-ray observation fields cover a large part of the *ISOCAM* survey (see Fig. 1-*right*): we know from *ISOCAM* if these X-ray sources have an IR excess (Bontemps *et al.* 1998). We restrict the following study to the *HRI/ISOCAM* common area. We have in this zone 55 X-ray sources, of which 47 are identified with an IR or optical stars, including 38 TTSs and 1 protostar classified from ground-based and *ISO* observation. There are also in this area 89 TTSs undetected with the *HRI*. In the next section, we will study the whole TTSs sample.

3. T Tauri Stars

3.1. X-ray and stellar luminosity correlation for T Tauri Stars

We have represented the X-ray luminosity of this sample versus the stellar luminosity (estimated from near-IR data in Bontemps *et al.* 1998). We have also estimated upper limits for TTSs undetected in X-rays.

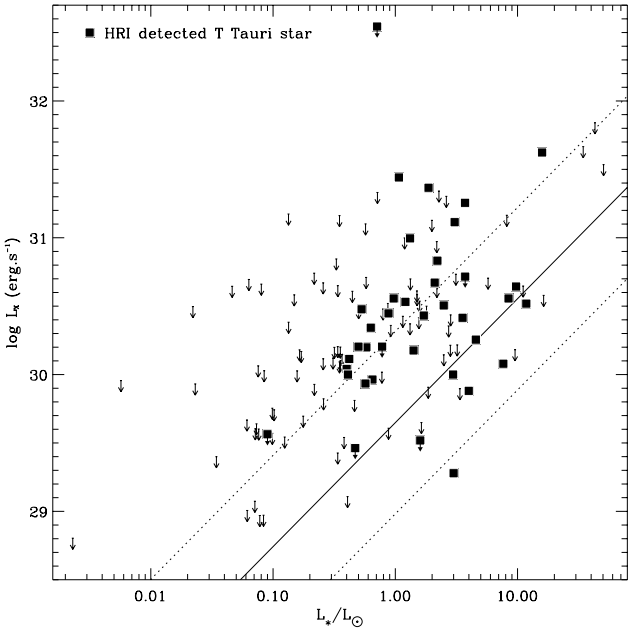

Fig. 2.— X-ray and stellar luminosity correlation for T Tauri Stars in the *HRI* sample.

We have tested with the ASURV statistical software package (Version 1.2 availabe at *http://www.astro.psu.edu/statcodes*), which takes upper limits into account, the probability that a correlation is not present. This probability is $< 10^{-4}$: we must have a strong correlation between X-ray and stellar luminosity. This correlation is given by ASURV: $\mathrm{Log}(L_X/\mathrm{erg.s^{-1}}) = (0.91\pm0.14) \times \mathrm{Log}(L_\star/L_\odot) + 29.65$. Taking into account the slope uncertainty, this correlation can be rewritten has a simple proportionality: $L_X/L_\star \sim 10^{-4}$, confirming the result found by Casanova *et al.* (1995).
We are now able to study the X-ray detectability of TTSs versus extinction.

3.2. X-ray detectability of T Tauri Stars versus extinction

We want to see whether our X-ray detections are biaised by extinction. Using the X-ray and stellar luminosity correlation, we can "predict" for each TTS its X-ray luminosity from its stellar luminosity (Fig. 3). We estimated the *HRI* detection threshold on and off-axis for our observation (77,182 sec), and the extinction curve, assuming a typical TTSs spectrum (kT_X=1 keV plasma with cosmic abundances and Raymond-Smith line emissivities; see Montmerle 1997). We see that the undetected TTSs are below the *HRI* detection threshold, or have high extinctions ($A_V > 20$).

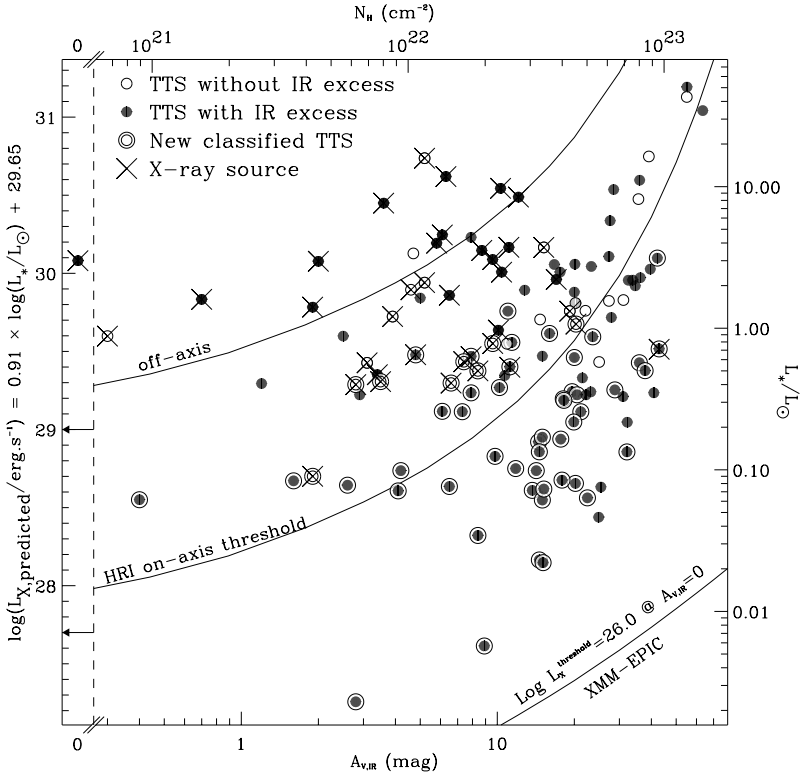

Fig. 3.— X-ray detectability of T Tauri Stars versus extinction: left scale: X-ray luminosity predicted from the $L_X/L_\star$ correlation; right scale: stellar luminosity $L_\star$ determined from near-IR photometry. The extinction is expressed both in N_H (top scale) and A_V (bottom scale). Curves show detection threshold for the *ROSAT HRI* (on and off-axis), and *XMM-EPIC*.

3.3. T Tauri Stars and XMM

Using X-rays we have detected new TTSs without IR excess, but we are limited by the extinction and our sensitivity (see Fig. 3). We can see that *ISOCAM* has detected a numerous new TTSs with IR excess, low stellar luminosity, and high extinction, which were not detected by *ROSAT* because too faint. We have estimated the *EPIC* detection threshold for the same exposure. *EPIC* thanks to the increase in sensitivity and the access to the 5-10 keV energy range will be able to detect all these new *ISOCAM* TTSs with IR excess. *EPIC* will also be able to distinguish within *ISOCAM* sources unclassified because without IR excess (not represented in Fig. 3), between field stars, low stellar luminosity TTSs without IR excess, and perhaps brown dwarfs.

4. Protostars

4.1. an X-ray Super-flare from an IR protostar

During our observation we detected X-ray emission from one protostar (Grosso *et al.* 1997). This protostar named YLW15, also called IRS43, is a well known core F IR protostar. IR protostars (Lada 1991) are according to current models, composite: they include a central star (still in the process of formation), surrounded by an accretion disk ∼10–100 AU in radius, and embedded in an extended, infalling envelope of gas and dust up to $\sim 10^4$ AU in size (Shu *et al.* 1987). This IR protostar was detected only in the first exposure. Its light curve showing an exponential decrease, was interpreted as post-flare cooling of a hot plasma. Because the *HRI* has no spectral resolution we assumed a wide range of temperature (1–6 $\times$ 10^7K), and estimated from the decay time the electronic density at the flare peak. We found typical solar coronal densities: 2–8 $\times$ 10^{10} cm^{-3}. With our best estimate for the extinction ($A_V \sim 30$), and assuming a Raymond Smith spectrum, we found an intrisic X-ray luminosity, integrated over all X-ray energies, $L^{bol}_{X,intrinsic} = 4 \times 10^{34}$–$10^{35}$ erg.s^{-1}, which is a huge luminosity compared to L_{bol}=10×$L_\odot$. Moreover, from the emission measure we estimated the loop length: l/$R_\odot$=35–25, which is big compared to typical TTSs loop length ($\leq$10 $R_\odot$). We are thus compelled to consider non-solar-type origins for the flare where the magnetic structure is connected to the disk, with a mechanism of explosive release of energy stored in magnetic fields through reconnection (Hayashi *et al.* 1996). In ρ Ophiuchi two or three others protostars were detected by *ASCA* (Kamata *et al.* 1997).

4.2. Protostars and XMM

Due to high extinction, detection of protostars with current satellites is difficult and rare. Only brightest events or less extincted protostars are detected. *ASCA* detects more X-ray emission from protostars than *ROSAT* thanks to its access to hard X-rays. With its 0.1–10 keV energy range, and its increase sensitivity, *XMM* will allow to make a breakthrough in protostar X-ray studies. We have simulated using XSPEC the X-ray emission from a ρ Ophiuchi protostar

(d=160pc), with $A_V = 30$ mag (N_H=6.7 $\times$ 10^{22} cm^{-2}), a Raymond-Smith spectrum with $T_X = 6$ keV, $L^{bol}_{X,intrinsic}$=10^{31} erg.s^{-1} (which is a minimal case), and a 25 ksec observation. This gives 13200 counts observed by *EPIC* (Fig. 4). In this simulation iron line profile is well resolved and distinctly shows the K_α and K_β lines. In a way reminiscent of obscured AGNs, *EPIC* will have capability to do spectral studies at high resolution, allowing detailed studies of the plasma composition and temperature(s), and of the extinction along the line-of-sight.

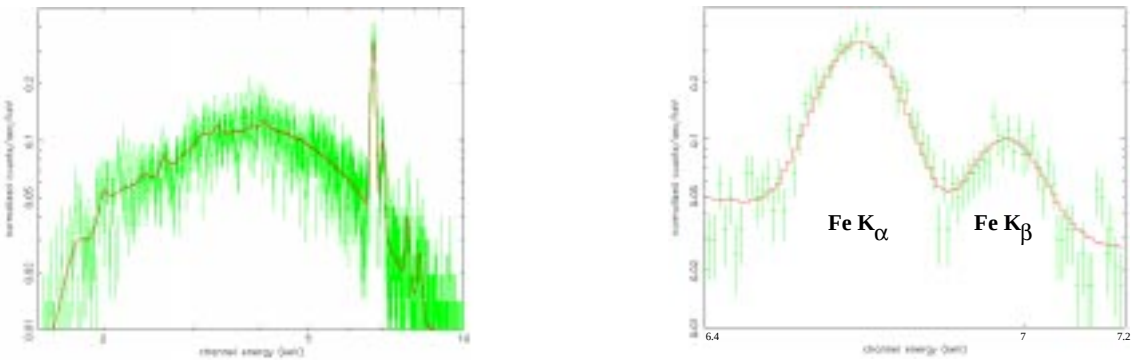

Fig. 4.— Simulation with XSPEC of the X-ray spectrum of a deeply embedded protostar observed with *EPIC* .

5. Conclusion

XMM will detect numerous population of embedded and low stellar luminosity TTSs and protostars. This will give a better knowledge of X-ray sources in regions of star formation. This knowledge is important because X-ray emission induces various effect on circumstellar and interstellar matter: stimulated accretion by disk ionization via coupling with magnetic field, interstellar medium ionization, heating and modification of gas chemistry and dust grain composition, etc... (see review by Glassgold, Feigelson & Montmerle 1998).

REFERENCES

Abergel, A., *et al.* 1996, A&A, 315, L329

Andre, P. & Montmerle, T. 1994, ApJ, 420, 837

Bontemps *et al.* 1998, A&A, *in preparation*

Canzian, B. 1997, CCD Astronomy, 4, 16

Casanova, S., Montmerle, T., Feigelson, E.D. & André, P. 1995, ApJ, 439, 752

Glassgold, A.E., Feigelson, E.D. & Montmerle, T. 1998, in *"Protostars & Protoplanets IV", in press*

Grosso, N., Montmerle, T., Feigelson, E. D., Andre, P., Casanova, S., & Gregorio-Hetem, J. 1997, Nature, 387, 56

Hayashi, M.R., Shibata, K. & Matsumoto, R. 1996, ApJ, 468, L37

Kamata, Y., Koyama, K., Tsuboi, Y., & Yamauchi, S. 1997, PASJ, 49, 461

Koyama, K., Ueno, S., Kobayashi, N. & Feigelson, E. 1996, PASJ, 48, 87

Lada, C. J. 1991, in *"The Physics of Star Formation and Early Stellar Evolution"*, NATO ASI, C.J. Lada & N.D. Kylafis, Kluwer, 329

Montmerle, T. 1997, IAU Symposia, 188, E4

Shu, F.H., Adams, F.C. & Lizano, S. 1987, ARA&A, 25, 23